Evaluation of Mixing Performance in Several Designs for Microfluidic Channel Mixers

왕양양† ·서용권* ·강상모**

Yangyang Wang, Yongkweon Suh and Sangmo Kang

Key Words : Microfluidics, Micro-mixer, Mixing index, Zeta-potential.

Abstract

We conducted a numerical study of AC-electroosmotic (alternating current) effect on the fluid flow and mixing in a 3-D microchannel. The microchannel used as an efficient micro-mixer is composed of a channel and a series of pairs of electrodes attached in zigzag pattern on the bottom wall. The AC electric field is applied to the electrodes so that a steady flow current takes place around the electrodes. This current is flowing across the channel and thus contributing to the mixing of the fluid within the channel. We performed numerical simulations by using a commercial code to obtain a steady flow field. This steady flow is then used in evaluation of the mixing performance via the concept of mixing index. It was found that good combination of two kinds of electrode, which gave us a good mixing, is not simple harmonic. And when the length ratio of these two kinds of electrode is 2:1, we can get the best mixing effect.

1. Introduction

Nowadays, microfluidic technologies find many applications in analytical and bioanalytical chemistry as well as synthetic organic chemistry. A lot of systems have been developed. These systems use a small space and have short diffusion distance and large specific interface compared with area. The microfluidic flow is always laminar. These characteristics promote highly efficient chemical reactions in a microchip while offering practical advantages like reduced sample and reagent volume. But, in these miniature scale devices, fluid mixing is particularly difficult. This is due to the fact that flows in micron sized straight channels with smooth walls are uniaxial and laminar, and occur at low Reynolds number and mixing in such flows is due to molecular diffusion alone. This necessitates the development of devices with high mixing capability.

† Dep. of Mechanical Engg. Dong-A Univ.
E-mail : dashifu2008@gmail.com
TEL : (051)200-6982 FAX : (051)200-7656

* Dong-A Univ.

** Dong-A Univ.

Various micromixers for rapid mixing of fluids have been reported during the past decade[1]. They can be classified into passive and active mixers. The former includes mixing by splitting and injecting of fluid flow into another flow[2], laminating thin layer flows[3], disturbing the fluid flow with microchannel structures[4], and confining the species in droplets[5]. In the case of active mixers, the fluids are stirred by external forces using ultrasonic[6], acoustic[7], magnetic[8], or electrical actuation[9].

Current and potential utilizations of microfluidics require that the solution design is simple to fabricate and use. So, we focus on the active mixers. In a similar spirit, the goal of the present study is to induce mixing in a straight microchannel. Indeed, one of the advantages of micro-electro-mechanical systems (MEMS) is that electric fields of relatively large magnitude can be generated by means of low voltages. The use of electric fields also avoids the introduction of moving components, which often cause a problem in miniature devices. In this paper, we propose mixers enhanced by alternate currency electro-osmotic flow (AC-EOF).

Utilization of AC-EOF is one attractive way to move a fluid in a small space such as a microchannel for the following reasons: (1) the device to induce AC-EOF can be fabricated by a relatively easy process compared to the micromixers mentioned above; (2) the velocity of AC-EOF is sufficiently enough for microchemical processes (over 100 μm s–1); and (3) it is easy to control the flow direction by the electrode configuration.

2. Theories of Electro-Osmotic Flow

At first, we introduce the charge relaxation time τ, which, for a fluid with continuous electrical properties, is equal to $\tau = \varepsilon/\sigma$, that is the ratio between the fluid permittivity ε and its conductivity σ. It measures the rate at which the free charges relax from the bulk of the fluid to the outer boundaries of a dielectric mass. The free charges relaxation time τ is approximately 3.6 × 10^{-6} s for distilled water and 0.68 s for corn oil. For an alternating electric (AC) field oscillating at frequency f, one can compare the charge relaxation time with the inverse of the electric field frequency f. This leads to the ratio of time scales: $T = \dfrac{\tau}{1/f} = \tau \times f$.

The flow of an incompressible and Newtonian fluid in presence of an electric field is governed by the Navier–Stokes equations consisting of the conservation of mass (or continuity) equation and the momentum equation:

$$\nabla \cdot \vec{V} = 0 \qquad (1)$$

$$\rho\left[\frac{\partial \vec{V}}{\partial t} + \vec{V} \cdot \nabla \vec{V}\right] = -\nabla p + \eta \nabla^2 \vec{V} + \vec{F}_e \qquad (2)$$

Where $\vec{V}$ denotes the velocity field and p refers to the pressure. Here, the action of the gravitational force has been neglected. In case of very small Reynolds number (Re <<1), the non-linear (inertia) term in the left hand-side of eqn. (2) can be neglected. The action of the electric field appears on the right-hand side of the momentum eqn. (2) as a force, $\vec{F}_e$, which takes the expression

$$\vec{F}_e = q\vec{E} - \frac{1}{2}E^2\nabla\varepsilon - \nabla\left(\frac{1}{2}\rho E^2\left(\frac{\partial\varepsilon}{\partial\rho}\right)_T\right) \qquad (3)$$

Where $\vec{E}$ denotes the electric field, q the density of the free electrical charges, and T the temperature. The first term, $q\vec{E}$, or electrophoretic component, is the Coulomb force per unit volume exerted by the electric field upon the free electric charges of density q. The second term, $-1/2\,E^2\nabla\varepsilon$, or dielectrophoretic force, is due to the force exerted by an electric field on a dielectric fluid. The action of the third term, $-\nabla\left(\frac{1}{2}\rho E^2\left(\frac{\partial\varepsilon}{\partial\rho}\right)_T\right)$, or electrostrictive force, is the gradient of a scalar and can be regrouped with the pressure term in the Navier–Stokes equations. Its role is usually negligible on the hydrodynamics of an incompressible fluid.

The consideration of the relative importance of the two first terms in the force of electrical origin (eqn. (3)) requires an estimate of the dimensionless parameter $T = \dfrac{\tau}{1/f} = \tau \times f$ previously introduced. If this ratio is much larger than 1, that is f >>$1/\tau$, the free electric charges do not have time to build up in the fluid, and therefore cannot be acted upon by the electric field. In this case, the first term $q\vec{E}$ is negligible and the second term, $-1/2\,E^2\nabla\varepsilon$, typically predominates. In all other cases including the case of a DC electric field, the term $q\vec{E}$ is usually the dominant term. In our case, f <<$1/\tau$, so, the term $q\vec{E}$ is the dominant term.

In this paper, we utilize the electric force described for the purpose of mixing two fluids. And, we use corresponding boundary velocity to simulate the model.

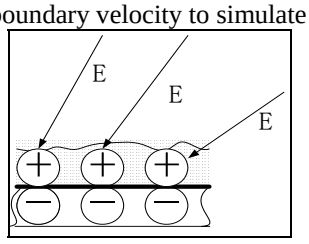

Fig.1. The schematic of charges and electric potential at surface of the electrodes

When an AC current is applied, the interfaces between the liquid and electrodes obtain a new distribution of ions, which is more than the ions caused by zeta potential. Because, there are some ions in the liquid, the moving of these ions changes the electric field to more flat. The

layers with charge against on electrodes move due to electric force, shown in Fig.1.

Since the boundary is impermeable, the layers of changes should obtain a velocity parallel to the channel walls.

So, the interfaces obtain a different velocity distribution, which is from the gap to the edge of the channel, shown in Fig.2.

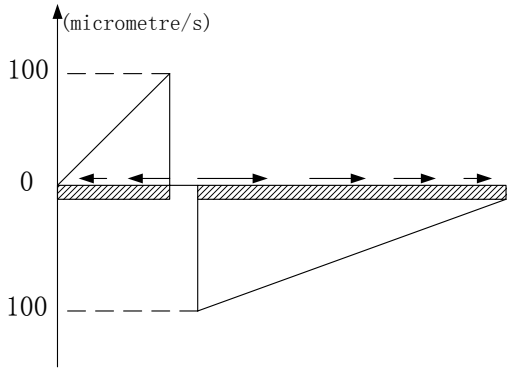

Fig.2. The velocity of a pair of electrodes caused by AC current

We use a linear boundary velocity distribution on the electrodes. Because the electric field caused by electrodes is strong near gap, and becomes weaker and weaker near the edges of the channel. The ions on the surface of gap is caused by zeta potential, the transverse velocity is much weaker, and we can consider that the transverse velocity at the gap equal to zero for easy simulation.

3. Numerical Method

Numerical simulation is performed by using a commercial code (CFX 10.0) on the basis of the implicit finite volume method. The calculation domain is shown in Fig.3.

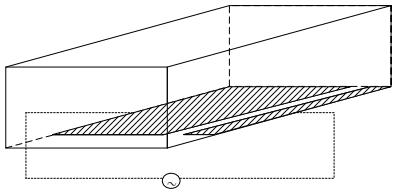

Fig.3 The calculation domain

The grid system is composed of hexahedron mesh with about 300000 grid points. The fluid is incompressible, and on the channel walls, the fluid is subjected to the no-slip, impermeable conditions and driven by considering pressure distribution, and these results are compared. In this study, water is chosen as the operating fluid.

At first we considered six shapes of electrodes which are attached to the bottom of the channel, as shown in Fig.4. The magnitude of AC potential applied to the electrodes is about 2V, and the frequency is 100Hz. We choose the velocity distribution corresponding to the condition.

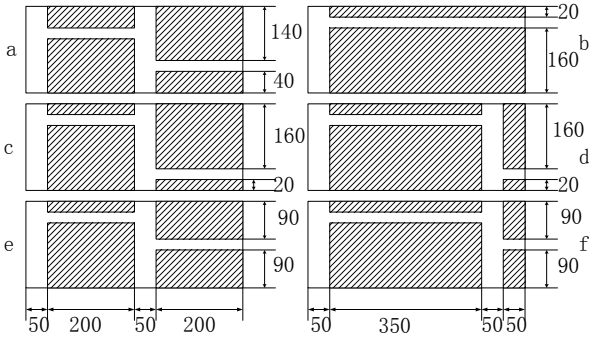

Fig.4. The electrode shapes

We used a periodic model to save time. In every calculation, we used pressure distribution to drive the fluidic in the channel; the magnitude is 150Pa/m.

To simulate the mixing effect in the channel, we add a new variable, the concentration of the species which is normalized to 1 in a half domain and zero on the other half domain. We utilize fine kinds of distributions of concentration as shown in Fig.5.

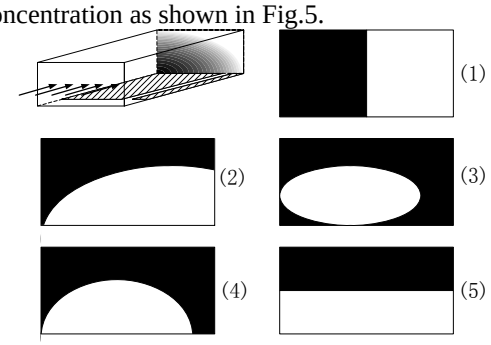

Fig.5. fine kinds of concentration distribution

The numerical simulation has been carried out for the diffusion coefficient of $D_d = 1\times10^{-12}\ m^2/s$, which is a typical value for an aqueous solution.

4. Results and Discussion

4.1 Comparison with Different Electrodes

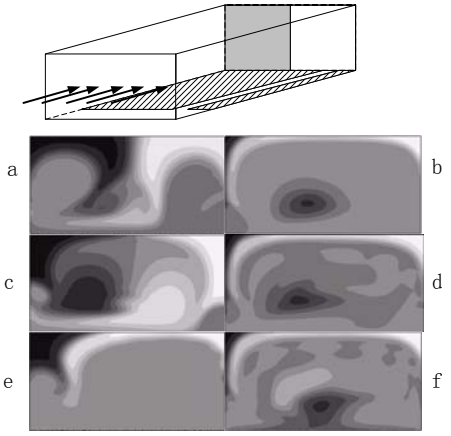

Fig. 6 The domain interface's concentration contours of model

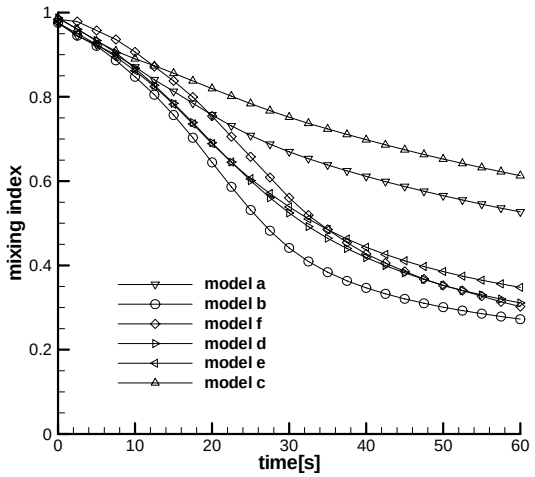

Fig.7. The mixing index of different models

We have compared the six models which have different shape of electrodes under the concentration distribution shown in Fig.5(1), and Fig.7 gives the comparison of the mixing index. The curve "a" corresponds to the model shown in Fig.4a, "b" corresponds to Fig.4b, "c" corresponds to Fig4.c, "d" corresponds to Fig4.d, and so on. It can be seen that the model shown in Fig.4b has best effect of mixing. The worst mixing is found in the model c which has a pair of zigzag electrodes. It is because the flow is laminar and the voltage applied to the electrodes is low. And under this low voltage, the short length of electrode in Fig.4c can't drive the flow in the channel sufficiently, and the two components of the zigzag electrodes weaken the affection of each other.

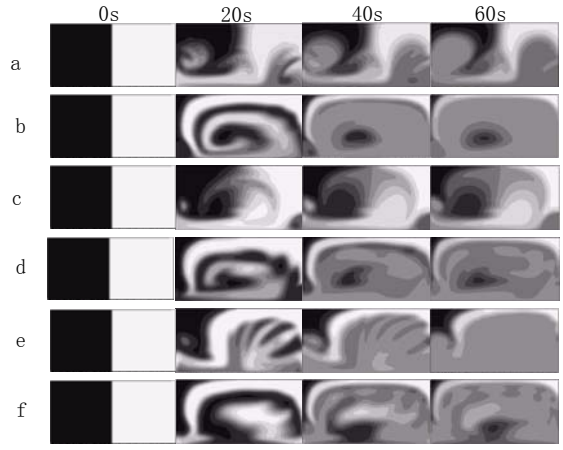

Fig.8. The concentration contour of different models, from upside to downside is corresponding to Fig.4a,b,c,d,e,f separately

Fig.8 shows the sections with concentration contour for different time. It is clearly see that the model e and f can give us longer interface. From Fig.8 we can see, at the beginning, the second model mixing was quick, and then the last two models' mixing became faster. It is because, after a few seconds, the last two models had longer interface in all models. So, we can imagine that, if the channel is a little longer, the last two models would give us a better mixing.

Practically, when microchannels are used in MEMS systems, the concentration distribution will be totally different. To make sure that how much does this change affect the mixing, we have changed the concentration distribution of the models shown in Fig4, and compared the final mixing index and the shape of concentration distribution of the section. The result is shown in Table.1 and Fig.9 separately.

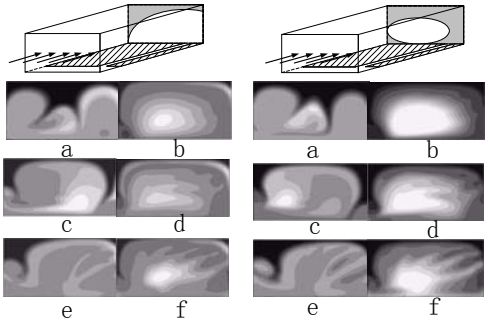

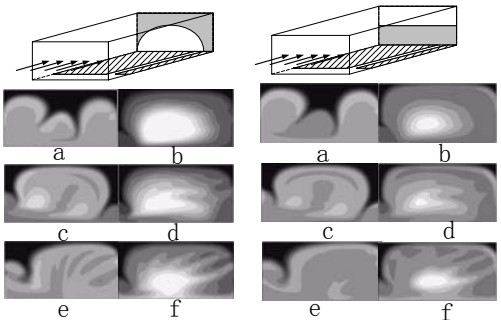

Fig. 9 The domain interface's concentration contours of models with different initial conditions when t=60s.

Fig.9 shows the contour of concentration of every model in different initial condition. It is clear that the model "e" and "f" always gave us the longest interface in three left models and three right models separately. To make this more evident, we compared the final mixing index in two groups, left models and right models of Fig.4, as shown in Table.1.

Table. 1 The comparison of final mixing index of every model with different initial conditions.

model / CD*	a	c	e	b	d	f
(1)	0.527	0.613	0.348	0.272	0.312	0.302
(2)	0.540	0.486	0.354	0.376	0.324	0.346
(3)	0.549	0.470	0.435	0.650	0.581	0.518
(4)	0.553	0.457	0.424	0.597	0.527	0.484
(5)	0.531	0.453	0.366	0.381	0.350	0.344

(CD*: initial concentration distribution)

Table.1 shows the comparison of channel with different electrodes and different initial concentration distributions. There are fine different concentration distributions and six different shapes of electrodes. Totally, we have thirty simulations to compare the mixing effect of models. It is clearly seen that, though the model shown in Fig.4b give us a good mixing under the concentration distribution shown in Fig.5(1), after we changed the concentration distribution, the mixing became worse. And we can see that, the shape of electrodes show in Fig.4e, Fig.4f always gave us a good mixing regardless different initial condition. We took out the common ground of these two models, and then we found that the component of the two pairs of electrodes is the same. The left pair is composed with a short electrode and a long one, the right pair is composed with two same electrodes.

4.2 Optimize the Best Combination of Pairs of Electrodes

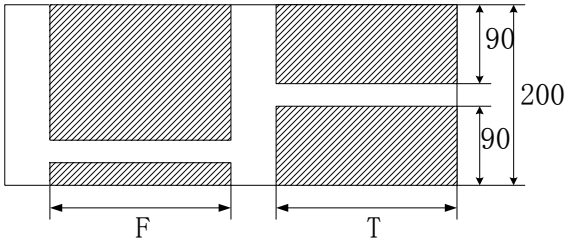

Fig.12 The best component of electrodes

In this part, we focus on the special combination of pairs of electrodes shown in Fig.12. We added two parameter "F" and "T", and then we compare the final mixing index of models with different "F:T", as shown in Table.2.

Table. 2 The final mixing index of the models with different F:T

F:T / CD*	1.00	1.50	1.86	2.08	2.33	3.00
(1)	0.348	0.292	0.285	0.282	0.281	0.293
(2)	0.355	0.298	0.282	0.277	0.277	0.294
(3)	0.435	0.394	0.389	0.390	0.396	0.424
(4)	0.424	0.382	0.373	0.372	0.375	0.396
(5)	0.366	0.325	0.312	0.309	0.310	0.344

(CD*: initial concentration distribution)

We can see that when the "F:T" close to 2, we can obtain better mixing. To make it clear, we compared the average mixing index of these models and got a curve shown in Fig.11.

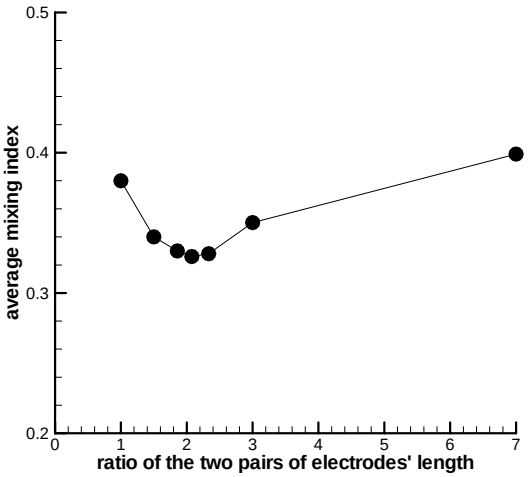

Fig. 11 Relationship between the average final mixing index and F:T

It is evidence that the best mixing effect is given by the model whose "F:T" equals to "270:130". About this model, the mixing index and contour of concentration distribution as a function of time are shown in Fig.12 and Fig.13, separately.

In Fig.12, we could see that the curve of mixing index, and then we contrast with the contour of corresponding time. It is clear that when the contour picture has little interface, the slope of the curve is small. In a word, we found that this model can provide large interface area regardless the initial condition of concentration. At the same time, it can give us the best mixing effect regardless the initial condition of concentration.

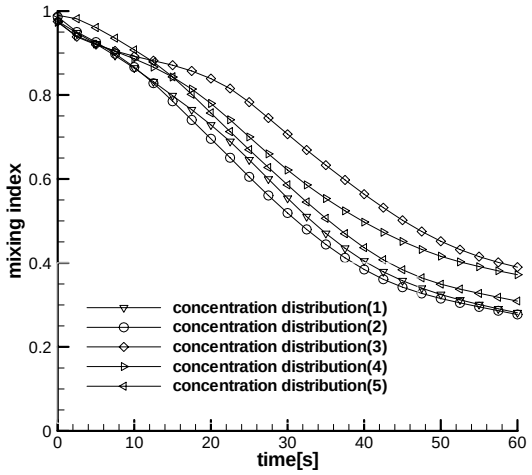

Fig.12 The mixing index of the optimum model as a function of time

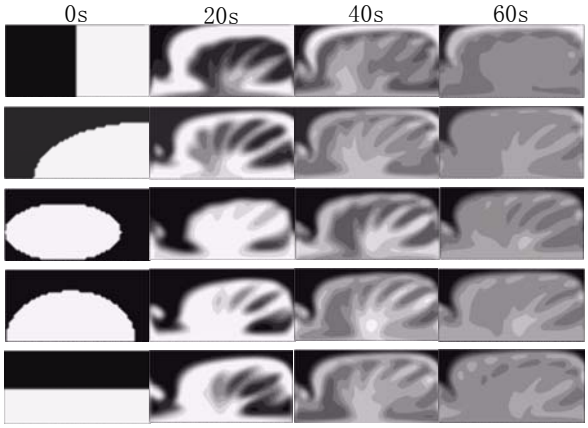

Fig. 13 The contour of concentration of the optimum model with different initial conditions.

5. Conclusion

In this study, we found that when the channel is short and under the concentration distribution shown in Fig.6(1), the best mixing obtained in the model shown in Fig.4b, and the benefit of the zigzag electrodes disappears. But when we changed the concentration distribution, the condition was totally different. And the benefit of the zigzag electrodes was returned. It was found that a special combination of two pairs of electrodes shown in Fig.10 can gave us a good mixing. And when the length ratio of these two pairs of electrodes is 270:130, we can get the best mixing effect.

Acknowledgements

This work was supported by the National Research Laboratory Program of the Korea Science and Engineering Foundation

Reference

(1)V. Hessel, H. Lowe and F. Schonfeld, Chem. Eng. Sci., 2005, 60, 2479

(2)R. Miyake, T. S. J. Lammerink, M. Elwenspoek and J. H. J. Fluitman, Proceedings of the 1993 IEEE Micro Electro Mechanical Systems—MEMS, Fort Lauderdale, FL, USA, 1993, p. 248.

(3)F. G. Bessoth, A. J. deMello and A. Manz, Anal. Commun., 1999, 36, 213

(4)A. D. Stroock, S. K. W. Dertinger, A. Ajdari, I. Mezic, H. A. Stone and G. M. Whitesides, Science, 2002, 295, 647

(5)K. Hosokawa, T. Fujii and I. Endo, Proceedings of the 1999 12th IEEE International Conference on Micro Electro Mechanical Systems, MEMS, Orlando, FL, USA, 1999, p. 388.

(6)M. Bengtsson and T. Laurell, Anal. Bioanal. Chem., 2004, 378, 1716

(7)R. H. Liu, R. Lenigk, R. L. Druyor-Sanchez, J. N. Yang and P. Grodzinski, Anal. Chem., 2003, 75, 1911.

(8)K. S. Ryu, K. Shaikh, E. Goluch, Z. F. Fan and C. Liu, Lab Chip, 2004, 4, 608.

(9)M. H. Oddy, J. G. Santiago and J. C. Mikkelsen, Anal. Chem., 2001, 73, 5822.